Frequency and spatial distribution of avulsion nodes on river deltas as a function of wave energy

A THESIS
SUBMITTED TO THE FACULTY OF THE GRADUATE SCHOOL OF THE
UNIVERSITY OF MINNESOTA BY

Julia Halbur

IN PARTIAL FULFILLMENT OF THE REQUIREMENTS
FOR THE DEGREE OF MASTER OF SCIENCE

Dr. John Swenson

July 2013

Table of Contents

List of tables

List of figures

1. Introduction

Deltas are created when a river meets a large body of water. Rivers carry sediment in their relatively fast flowing water and as the channelized flow moves into the more stationary water of a lake or ocean, the flow expands as a jet and the sediment-laden water decelerates and drops out the sediment load. This supply of sediment leads to a net depositional system that is one of the basic constructional units of sedimentary basins. By definition, deltas consist of subaerial (delta topset) and subaqueous (delta foreset and bottomset) environments. In a bulk sense, deltas accumulate sediment eroded off the continental land surface and incorporate it by aggrading the surface of the delta – growing in height – or expanding (prograding) the edges of the delta out into the body of water. Sediment deposited on the delta topset is sorted by fluvial processes; the coarser particles – sand and gravel – accumulate in the channels and their proximal levees while the finer particulates – silt and mud – create floodplain deposits. Most deltas worldwide are located on continental margins, where subsidence of the Earth's crust allows for long-term accumulation of sediment to form sedimentary basins. Due to this subsidence, some of the incoming sediment supply is solely used to maintain the elevation of the delta, but if there is additional material, it can be used to increase the size of the delta via progradation. The three fundamental controls on the rate at which a delta grows are sediment supply, subsidence, and changes in eustatic sea level. Marine processes – waves, in particular – redistribute sediment on the delta front (delta foreset and bottomset). In a general sense, the waves 'smear' the sediment delivered by channels to the delta front which creates a smoothing of the delta morphology in map view. This study focuses on the interplay of two important factors: The amount of sediment being

supplied to a given delta and the wave energy that is affecting that delta, which is mainly a function of the climate.

Sediment is distributed across the surface of a delta by a number of distributary channels. These networks of distributary channels are not constant in space and time, but move around based on channel dynamics and differences in elevation from one area of

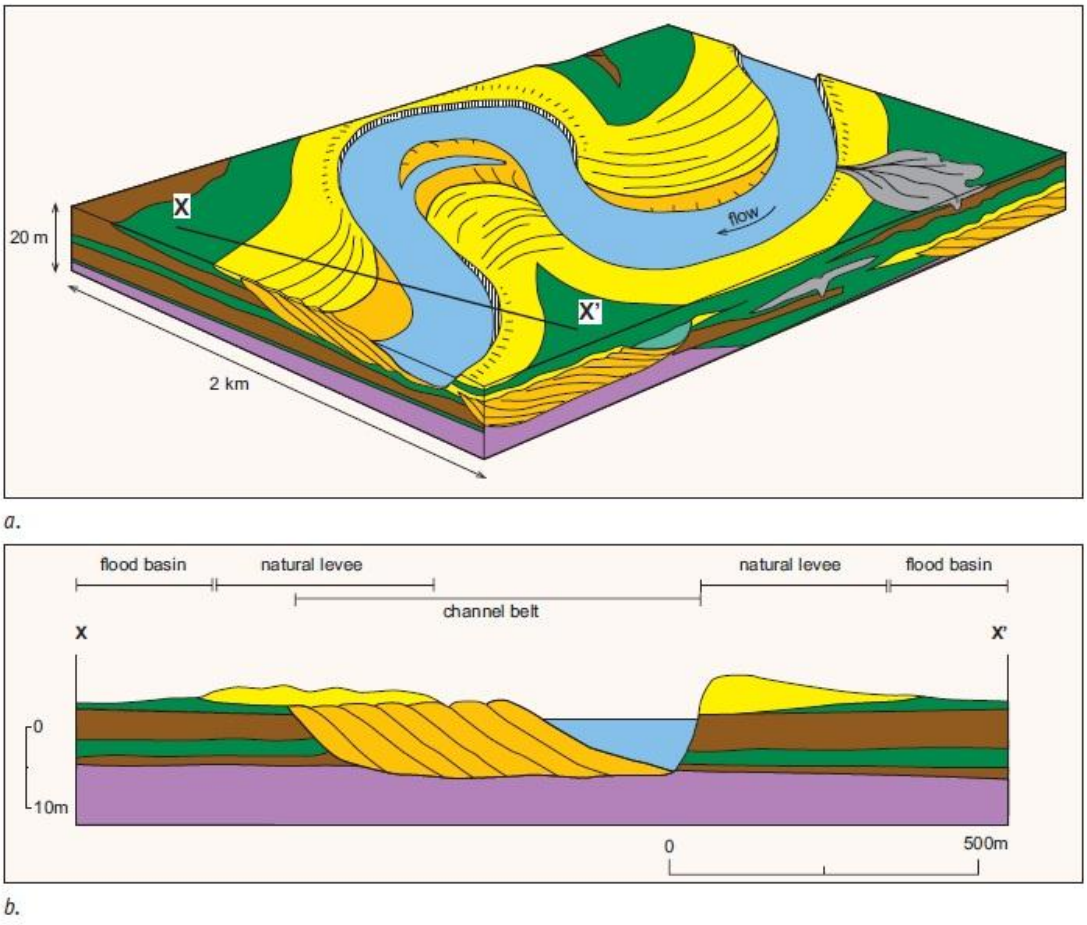

Figure 1. An example of channel migration with erosional cut banks and depositional point bars (Gouw, 2007).

the delta to another. Two distinct ways channels move around on the surface of a delta are channel migration (Figure 1) and avulsions (Figure 2). Channel migration occurs as the river erodes sediment on cut banks on the outside of bends and deposits it as point bars on the inside of bends. This process slowly moves the channel continuously across

the surface of a delta, leaving in its wake a series of accretion sets and scroll bars (Figure 1). Avulsions, on the other hand, occur basically instantaneously – at least on a geologic timescale. An avulsion occurs when the channel becomes super-elevated with respect to the surrounding floodplain and the resultant gravitational instability causes the river to change course abruptly to achieve a state of lower potential energy. Super-elevation of the channel results from the enhanced deposition of sediment in the channel levees and on the channel bed relative to the surrounding floodplain and is a function of how much sediment is being carried by the channel. In map view, the signs left behind by these two processes are vastly different. In the case of channel migration, the dominant features left behind are the previously mentioned scroll bars, continuous systems of depositional features, which show where the channel has been. The 'scars' left behind by avulsions are simply empty channels where relatively little water is flowing. The relict channels are typically filled with water, but they transport very little sediment compared to the active channels. Through time, relict channels are filled by floodplain deposition. These scars, or relict channels, provide a means for determining where the channel has been in the relatively recent (geologic) past and can be used to constrain the frequency of avulsions: In a gross sense, a delta with abundant channel scars has a relatively high frequency of avulsion.

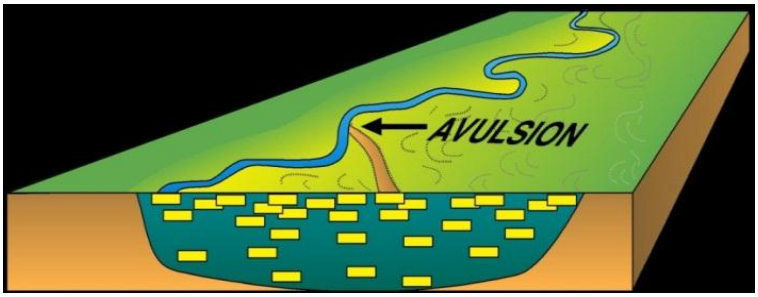

Figure 2. An example of an avulsion as well as a cross section of the preserved channels in the substrate (figure from Paul Heller).

A delta has a large surface area relative to the area of the channels that are supplying it with sediment and, thus, the channels can be envisioned as line sources of sediment that have to distribute their load across the entire delta surface to counteract subsidence and keep the delta from drowning. To do this, the channels have to move around, and avulsions are the principal method for achieving rapid movement of distributary channels. As avulsions are the dominant process operating on the surface of the delta, they are also the dominant control on what is preserved in the sedimentary record, or stratigraphic architecture, beneath the surface of the delta. Sand bodies created by deposition of sediment in a channel and the ensuing abandonment of that channel form important elements for the storage of subsurface fluids: When buried, channels from a delta surface produce relatively permeable sand bodies in the subsurface that are surrounded by relatively low permeability floodplain deposits; these sand bodies can potentially be preserved in the rock record as reservoirs. The frequency of avulsions on the delta surface controls the density of reservoirs and their interconnectivity. Hence, by better understanding the controls on the frequency of avulsions, locations of subsurface sand bodies from ancient systems – ideal reservoirs for groundwater and hydrocarbons – can be better predicted.

1.1 Avulsions

Avulsions themselves are not well understood due to the internal dynamics that arise from the complex interaction between water (channelized flow) and sediment (the mobile channel bed and the surrounding floodplain). While avulsions are often considered instantaneous on geologic timescales, the process of 'completing' an avulsion

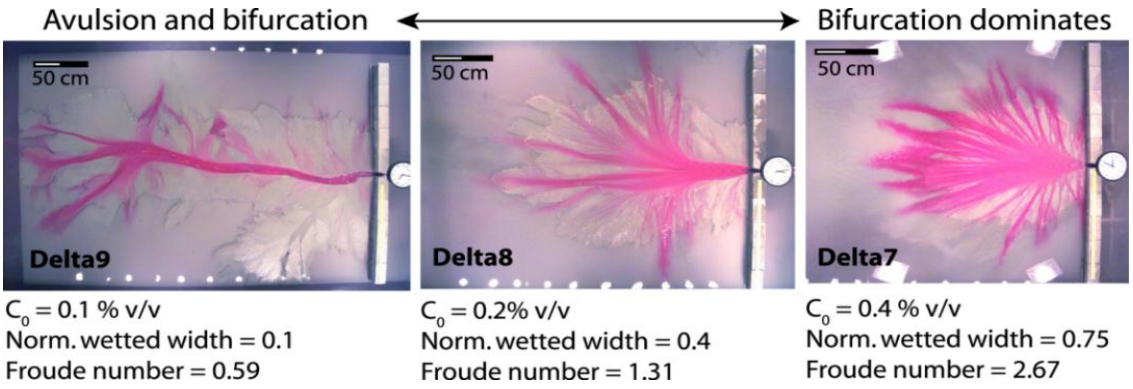

Figure 3. A laboratory model of a channel with varying sediment concentration which leads to different avulsion frequencies (Hoyal and Sheets, 2009).

generally requires decades to centuries, making them a difficult phenomenon to directly observe. Avulsion dynamics are stochastic and occur over 'meso' timescales greater than the shaping of a channel via bar forms and shorter than timescales associated with deposition from subsidence (Sheets, 2002). Laboratory-scale models of avulsions have been attempted (Figure 3), but the dynamics of sediment/water interactions – particularly the dynamics of floodplains – are difficult to scale down (Hajek and Wolinsky, 2011; Hoyal and Sheets, 2009; Sheets, 2002).

The avulsion process is thought to consist of two distinct components: A long-term 'setup,' which involves the systematic increase in elevation of a channel with respect to its surrounding floodplain, and the 'trigger,' which is the actual event that initiates the

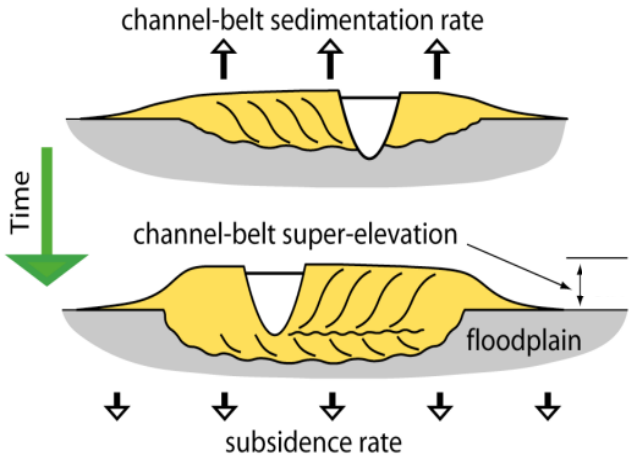

Figure 4. The idea of super-elevation. Note that sedimentation increases the elevation of the channel walls until they are approximately equal to the channel depth above the floodplain.

process of flow rerouting. Two threshold conditions have been proposed that, when destabilized by a trigger, result in an avulsion (Slingerland and Smith, 1998; Slingerland and Smith, 2004). The first involves the ratio of the lateral slope of the channel levees to the slope of the long profile (Mackey and Bridge, 1995); when this slope ratio exceeds a threshold criterion, avulsion occurs. The second condition focuses on the local super-elevation of a channel leading to a gravitational instability (Mohrig et al., 2000). Based on a combination of theory and rigorous field observations, Mohrig et al. (2000) proposed that as a channel deposits sediment on its bed and in its channel levees, it aggrades (increases in elevation) until it becomes perched above the surrounding floodplain (Figure 4). Mohrig et al. (2000) found that in order for there to be enough potential energy for an avulsion to proceed, the elevation of the channel bed had to be similar to the elevation of the floodplain – in other words, the difference in elevation scaled with the flow depth. Once it reaches this critical point, the channel is primed for a trigger to initiate the avulsion process. Figure 5 shows the perched nature of the channels of the Assiniboine River 'delta' that forms where the river crosses a significant topographic step and becomes strongly depositional. Both the active channels as well as the abandoned channels are higher in elevation than the surrounding floodplain due to the sediment

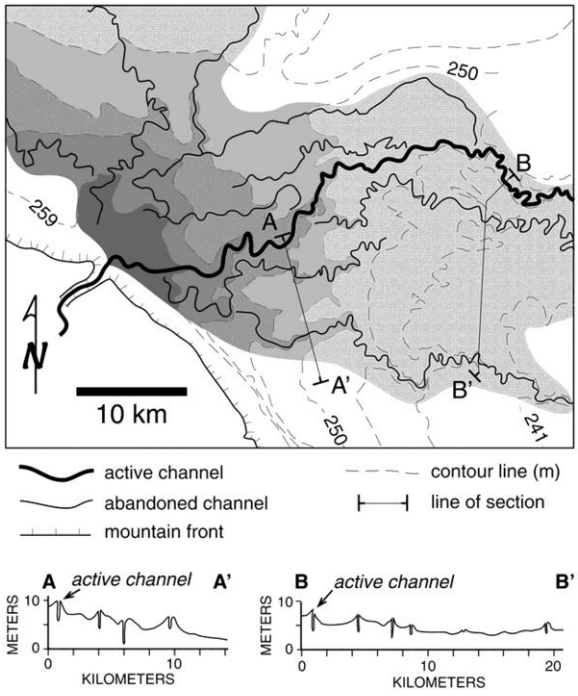

Figure 5. Map view and cross sections of the 'delta' on the Assiniboine River, Canada (Mohrig et al., 2000).

deposition in the channel levees. The active channel is perched higher than any of the relict channels while the elevations of the relict channels decreases with their age – the oldest relict channel is lowest.

It is worth noting that the two threshold conditions are basically the same, as they both conclude that an avulsion happens when the ratio of the cross channel slope to the down channel slope reaches a critical value. The community as a whole has largely adopted the Mohrig et al. (2000) super-elevation criterion for avulsion setup.

If the idea of super-elevation as the basic control on avulsion holds, avulsions could, in principle, occur anywhere on the surface of a delta. Surprisingly, few studies have considered the spatial distribution of avulsions on a delta surface. Jerolmack and Swenson (2007) mapped active channels on a relatively small set of modern deltas to illustrate how distributary networks on a delta surface evolve. They focused on two processes – avulsion and mouth-bar-driven bifurcation – to create a conceptual model of delta growth. Interestingly, Jerolmack and Swenson (2007) found that avulsion seems to generate only large distributary channels with length scales comparable to the overall dimensions of the delta. Initially, this finding would suggest that avulsions do not operate across the entirety of the delta surface and, instead, are focused near the delta apex. However, Jerolmack and Swenson's (2007) mapping strategy ignored relict channel segments – they only mapped the active channels, and therefore, failed to capture evidence of geologically-recent avulsions in the delta surface. Had they mapped these relict channels, perhaps they would have found a more uniform distribution of avulsion sites across the delta surface. One of the primary goals of this study was to determine whether or not avulsions operate across the entire surface of the delta.

Triggers for avulsions generally occur in the form of a flood, but can be any event that increases the discharge in the river enough to overcome the 'sticking point' and initiate the processes that move the channel to a lower elevation. After the river avulses onto the lower elevation of the floodplain, it leaves behind a characteristic channel scar. Though instantaneous on geologic timescales, this process can occur over decades, with the channel 'toggling' between its 'old' and 'new' configurations on annual timescales before ultimately selecting the 'new' (lower) configuration. Thus, the splitting of flow between channel branches at an active bifurcation could be envisioned as an avulsion in action; only continuous observation for decades would resolve whether or not the bifurcation was truly stable.

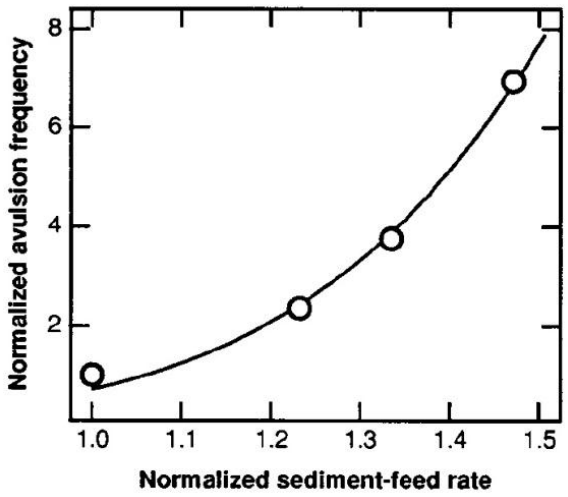

Figure 6. Plot comparing avulsion frequency with sediment supply rate in an experimental setting (Bryant, 1995).

There have been a number of studies dedicated to looking at controls of avulsion frequency. Universally, these studies focused on the more traditional controls on avulsion such as bulk sedimentation rate (a measure of relative sediment supply) and subsidence (Figure 6) (Bryant, 1995; Heller and Paola, 1996; Ashworth, 2004); other studies addressed the role of changing relative sea level in affecting avulsion frequency (Stouthamer, 2007; Shanley and MaCabe, 1994; Slingerland and Smith, 2004; Martin et al., 2009; Tornqvist and Bridge, 2002). Few, if any, studies have taken into consideration the possibility of a downstream control on avulsion frequency other than relative sea

level, though it has been shown through both observation and modeling that waves and tides dramatically affect the morphology of deltas (Figure 7) (Wright and Coleman, 1973; Galloway, 1975). Given the effects they have on the shape of a delta, it is possible that waves and tides could influence channel dynamics, and thus, avulsion processes as well. Swenson (2005) considered the potential for waves to hinder avulsions by predicting that an important control on avulsion frequency is the ratio of wave energy to fluvial input of water and sediment. This study attempted to test this idea.

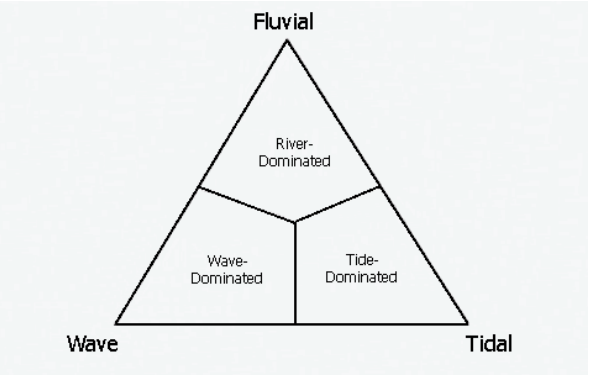

Figure 7. Ternary diagram with the major allochthonous controls on delta morphology (after Galloway, 1975).

1.2 Objectives

My study had two primary objectives. The first was an attempt to test the hypothesis of Swenson (2005), which states that an increase in wave energy should reduce the avulsion frequency of distributary channels. This test involved mapping relict channel scars and bifurcations on satellite images of modern deltas. In the following section, I discuss the concept of how waves might suppress avulsions and then outline a mathematical model of this basic idea.

The second objective was to directly measure the spatial distribution of avulsions on delta surfaces; in doing so, I addressed a basic consequence of the Mohrig et al. (2000) super-elevation setup criterion, namely that avulsions can happen anywhere on the delta

surface where the channel super-elevates sufficiently. A related goal was to determine how waves might affect the spatial distribution of avulsions. For this second objective, I used the same set of deltas as in the first objective.

2. Wave-driven suppression of avulsion frequency

2.1 Conceptual model

Swenson (2005) introduced the simple idea that wave energy plays an important role in determining avulsion rates because it controls how much sediment is being

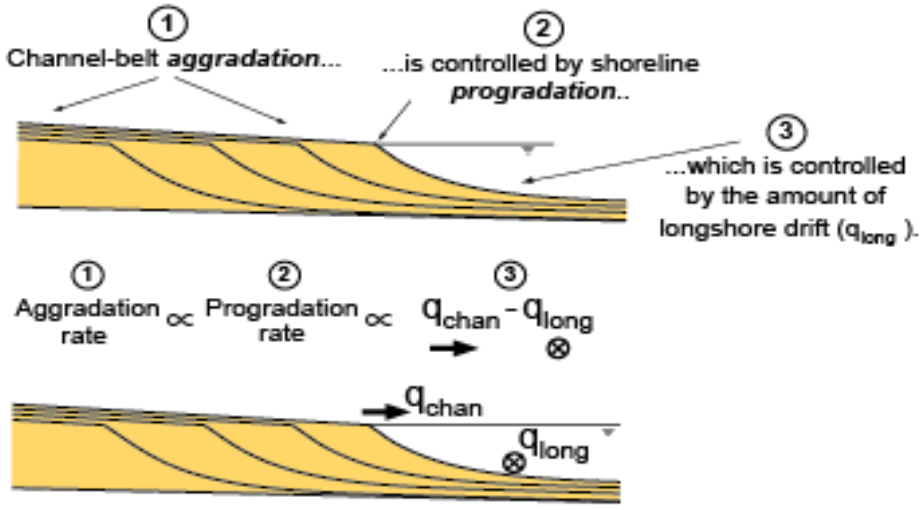

Figure 8. Schematic describing the location and controls of sediment deposition (Swenson et. al, 2006).

removed from the distributary channel system and thus not being used to aggrade the channel. Consider a single distributary channel. In the channel, sediment and water are transported due to the slope of the system, which tends to remain fairly constant through time. Thus, as the elevation of the channel long profile is increasing – as it is aggrading – the length of the channel must increase as well in order for a deltaic system to maintain

its slope. In cross section, the channel profile extends seaward in a self-similar fashion and, roughly speaking, a unit of channel progradation corresponds to some geometrically-constant unit of channel aggradation (Figure 8). The rate of progradation is controlled by the sediment supply reaching the channel terminus and the water depth of the delta foreset. In a system with no wave influence, the progradation rate is maximized because the sediment supply reaching the channel tip is all deposited on the foreset and, thus, used to prograde the channel tip out into the body of water. If there is wave energy, the process becomes more complicated. In the form of longshore drift, waves move sediment away from the channel tip, reducing the amount of sediment available to deposit on the foreset and drive the tip seaward. As a result, wave energy reduces the rate at which the channel tip progrades; by geometry, this reduced progradation rate translates into a reduced aggradation rate. More wave energy leads to less super-elevation which leads to a longer time interval between avulsions; thus, the more wave energy affecting the delta, the lower the avulsion frequency.

2.2 Mathematical model

Swenson (2005) constructed a mathematical model of the above conceptual model; in this section I synthesize the basic elements of this model. The goal of the model was to couple a model of channel long-profile dynamics to a model of beach evolution via longshore transport, both of which hinge on the diffusive processes of deltaic systems. Longshore transport as it affects shoreline dynamics has been treated diffusively (Komar, 1973); likewise, the morphodynamics of channel belts (long profiles) has also been considered a diffusive process. By combining these two one-dimensional

systems and coupling them at the channel terminus, this model predicts that effects on the morphology of the delta can be observed in aspects of the channel dynamics (Figure 9). Some basic assumptions made when applying this model are: The sand and water supply as well as the climate are all steady; the channel belt and shoreface are composed of sand while the floodplain is made completely of mud; the channel has a fixed width and the shoreface a fixed geometry; and there are no tides or changes is eustatic sea level.

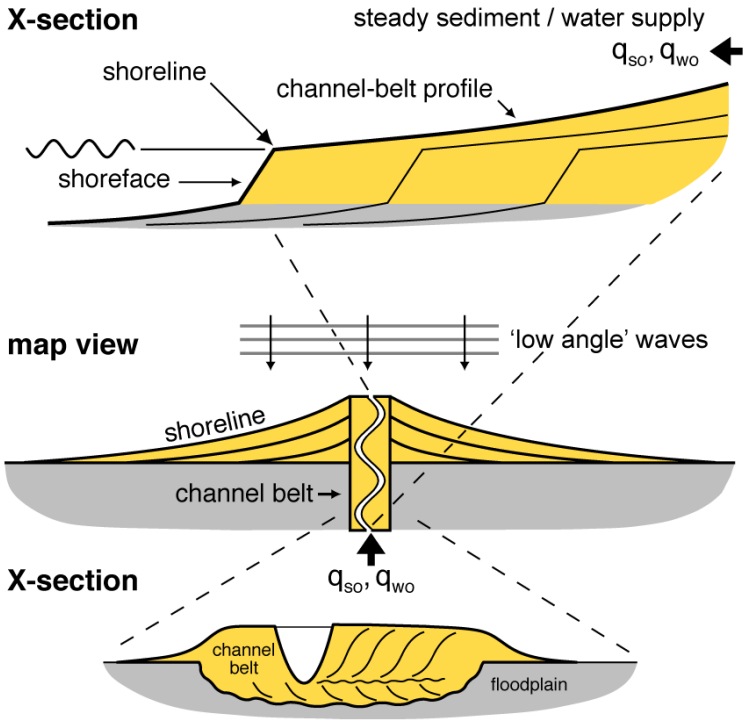

Figure 9. Simplified figure of the coupling between a channel belt and the morphology of a delta.

One of the two basic premises of this model is that channel belt morphodynamics are diffusive (Figure 10). The sediment flux (q_s) is proportional to slope in the channel:

$$q_s = -\nu \frac{\partial \eta}{\partial x} \qquad (1)$$

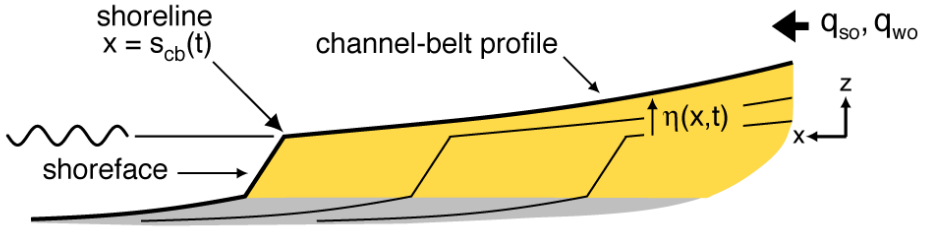

Figure 10. Long profile of a channel belt.

where η is the channel elevation and v the channel belt diffusivity, which is mostly a function of the water supply in the system (Paola, 2000; Swenson et al., 2000). Conservation of sediment volume tells us that the change in sediment flux over distance is proportional to the sedimentation rate, i.e. the change in channel elevation with time:

$$\frac{\partial q_s}{\partial x} = -\frac{\partial \eta}{\partial t} \tag{2}$$

Combining these two equations results in the diffusion equation that relates the change in channel elevation with time to the second derivative of the channel elevation with respect to position, i.e. the channel-belt curvature:

$$\frac{\partial \eta}{\partial t} = \nu \frac{\partial^2 \eta}{\partial x^2} \tag{3}$$

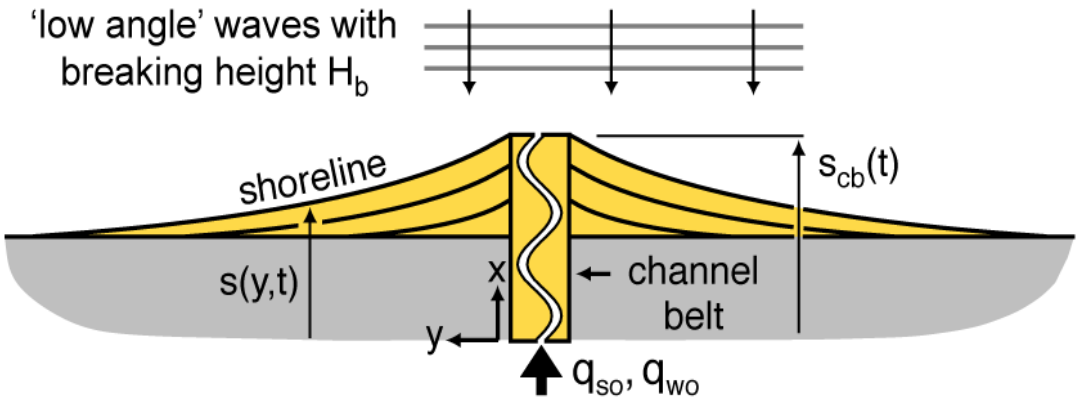

Figure 11. Map view of a channel entering a body of water.

Much of the same physics applies to the mathematical modeling of shoreface morphodynamics (Figure 11). The longshore sediment supply is proportional to the distance to the edge of the delta with respect to the distance away from the channel, i.e. the sediment flux varies with the map view 'slope' of the shoreline (Figure 11):

$$q_s = -\kappa \frac{\partial s}{\partial y} \tag{4}$$

where κ is the shoreface diffusivity, which depends on the wave amplitude. Again, conservation of sediment volume tells us that the change in sediment supply over space is proportional to the progradation rate of the shoreface:

$$\frac{\partial q_s}{\partial y} = -\frac{\partial s}{\partial t} \tag{5}$$

This results in a diffusion equation similar to that of channel belt morphodynamics:

$$\frac{\partial s}{\partial t} = \kappa \frac{\partial^2 s}{\partial y^2} \tag{6}$$

Equations (3) and (6) should be simple to solve; however, the position of the channel tip is unknown – it is a dependent variable in the problem. The above system of equations represents a moving-boundary problem (Swenson et al., 2000); an additional boundary condition that describes the coupling between the channel and the shoreface is required to

find a solution. In the following paragraph, I describe this coupling condition graphically.

By coupling these two diffusion equations at the channel tip, the shoreface is able to communicate with the channel belt. The left panel in Figure 12 shows the map view of

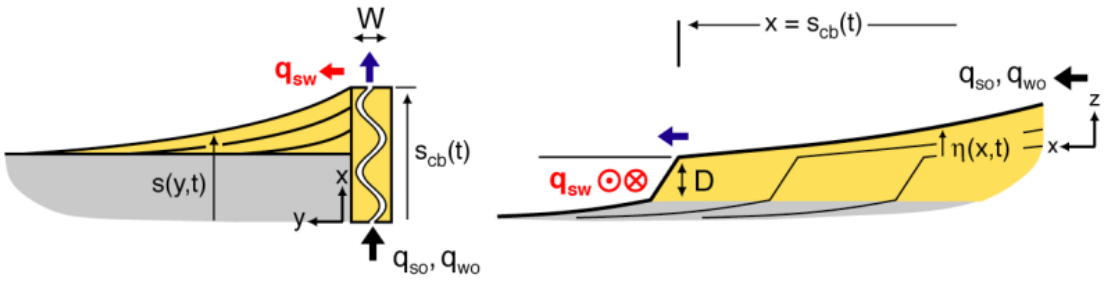

Figure 12. Coupling of the shoreface (map view) and channel belt (long profile) (Swenson et. al, 2006).

the shoreface, whereas the right panel shows the channel long profile and the shoreface cross section. In the left panel, the black arrow is the amount of sediment entering the system upstream. By Equation (3), some of the upstream sediment supply is deposited in the channel belt, which allows the channel to aggrade. The sediment flux reaching the channel tip is the sum of the blue and red arrows. When the red arrow – the sediment being moved away from the terminus of the channel by waves – is smaller than the blue arrow – the sediment available for

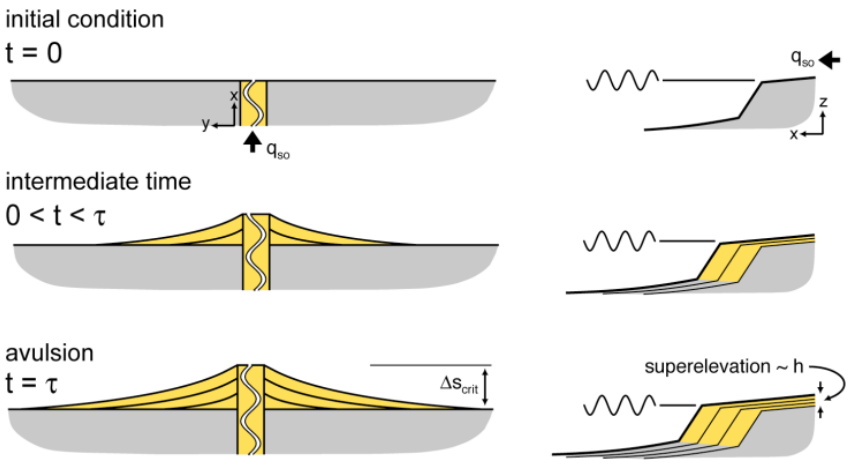

Figure 13. Progression of a channel building out into a body of water until it reaches the point of super-elevation. Map view on the left, cross section on the right.

progradation – the end of the channel will prograde into the body of water. The right panel shows the same concept, but in cross section. The rate at which the channel tip progrades is a function of the difference between the sediment flux reaching the channel tip and the flux extracted (smeared alongshore) by waves. Increasing wave energy reduces this difference by increasing the longshore flux, thereby reducing the rate of progradation and, correspondingly, channel aggradation.

Rather than working with avulsion frequency, the model actually predicts the channel residence time (τ), which is proportional to the multiplicative inverse of the avulsion frequency. Instead of quantifying how often a channel moves, it describes how long a channel stays in one location before moving. As a channel remains in one location, it builds up a cusp at the water interface until it reaches the super-elevation necessary for avulsing (Figure 13). Using geometry, the super-elevation necessary for avulsion, which scales with the flow depth (h), can be related to the critical progradation distance (Δs_{crit}) (Figure 14) in the equation:

$$\Delta s_{crit} \sim \frac{h}{S_o} \tag{7}$$

The characteristic slope of the channel (S_o) incorperates the sediment and water flux through diffusion. The backwater length of a fluvial system is also represented by h/S_o;

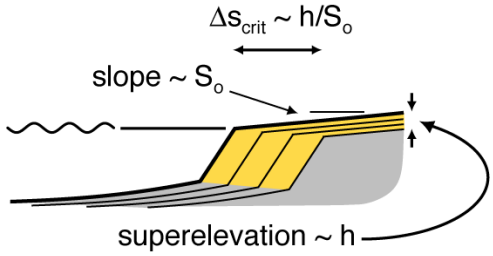

Figure 14. Schematic pointing out the relevant quantities for Δs_{crit}.

therefore, the model predicts that the channel belt should prograde to a distance that *scales like* the backwater length before an avulsion occurs.

A sand budget for a given system has three main components, the material being added to the system while the channel is in that location, the sediment being used for aggradation, and the sediment being smeared via longshre drift:

$$Q_{so}\tau \sim Br(R_{cb}\tau) + Ds_o\sqrt{\kappa\tau} \quad (8)$$

where Q_{so} is the sediment discharge, B is the width of the channel, r is the bulk delta radius, R_{cb} is the channel-belt sedimentation rate, D is the shoreface closure depth (approximately the depth of breaking waves), s_o is the progradation distance at which avulsion occurs (equivalent to Δs_{crit} in Equation 7), and κ is the 'diffusivity' of longshore transport (a function of wave energy) (Figure 15). Applying dimensional analysis to Equation (8), we find that the channel residence time, τ, is primarily a function of the river input and the wave energy:

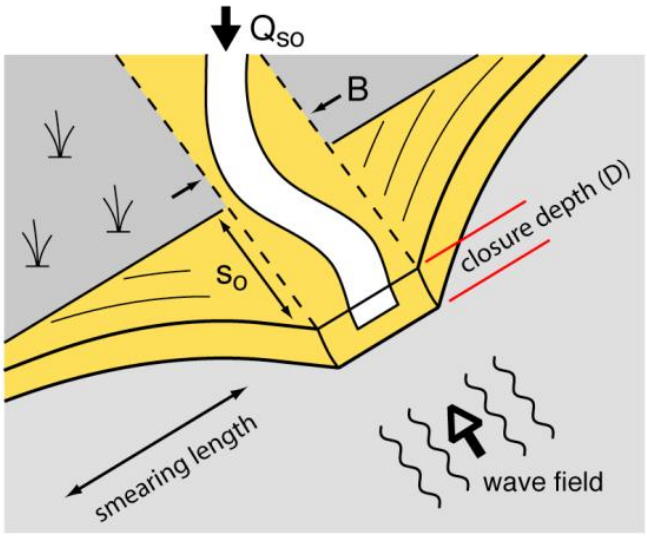

Figure 15. Cartoon illustrating the parameters contained in the sand budget.

$$f(\xi) = \frac{\tau}{\tau_o} \tag{9}$$

where ξ is a dimensionless parameter grouping that encapsulates the river and wave parameters and τ_o is an avulsion time scale set by the geometry of the channel belt. In a general sense, ξ is the ratio between the amount of wave energy and the fluvial sediment input.

$$\xi = \frac{\text{Wave parameters}}{\text{River parameters}}$$

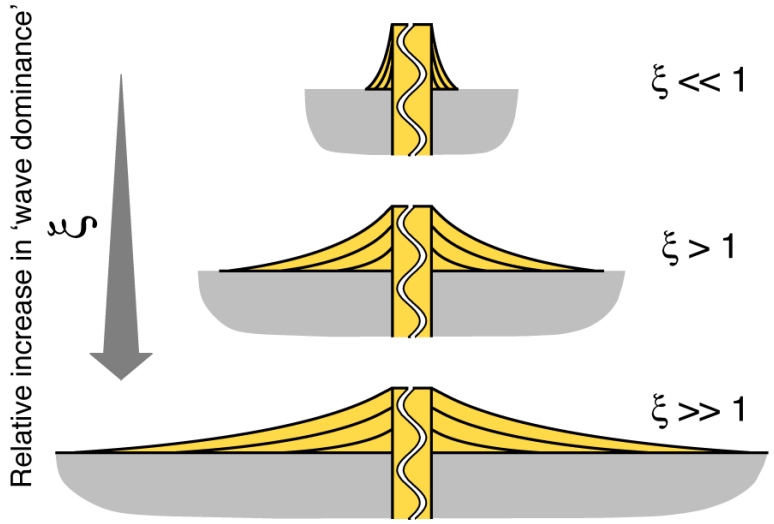

Figure 16. An example of difference delta geometries and their corresponding ξ values.

Systems that have a relatively high ξ value are ones where the wave energy far exceeds the fluvial input while systems with less wave energy have much smaller ξ values (Figure 16). In detail, the structure of ξ is:

$$\xi = \frac{DB}{Q_{so}}\sqrt{\frac{\kappa\sigma}{h}} \tag{10}$$

where σ is the subsidence rate. The effects of waves are embedded in the 'shoreface diffusivity' (κ); the remaining parameters describe fluvial input of sediment and water in the presence of subsidence.

Systems with a high value of ξ – abundant wave energy – have a longer τ as it takes more time to build up the channel to the point of an avulsion. This suggests that systems with more relative wave energy – compared to fluvial input – have fewer avulsions overall (Figure 17). Because the dimensionless number ξ represents the sediment and wave energy affecting a given delta, it also contains within it information about the basic (bulk) morphology of that delta. Deltas with relatively high ξ values are strongly influenced by waves; thus, their overall morphology should be smoothed and cuspate. In contrast, deltas with low ξ values would be considered more river dominated and should display a 'rougher' morphology, with distributary channel tips extending seaward. Therefore, as ξ embodies both the morphology of a delta and the channel residence time, which is directly related to the avulsion frequency, the overall morphology – something 'measured' with relative ease – can then be used as a proxy for ξ itself. In other words, the overall delta morphology can serve as a proxy for ξ, which itself is extremely difficult to constrain in natural systems.

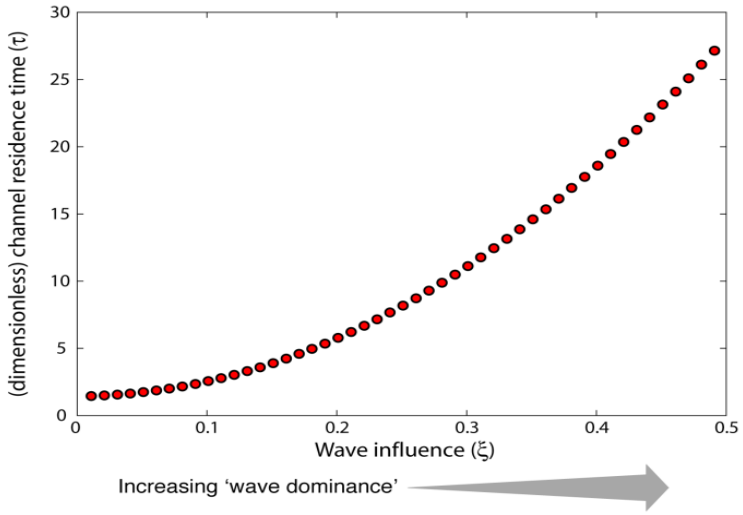

Figure 17. Results from Swenson (2005) model predicting more wave influence corresponds to a longer residence time.

Combining this idea with the above model, we would expect that deltas with a lot of wave energy – a high ξ value and a longer residence time – would have fewer scars than deltas that experience a smaller amount of wave energy. The longer a channel has to sit in one location before it can avulse, the more time the rest of the delta has to anneal – to fill in relict channels. Hence, deltas with high ξ values have a wave-dominated morphology, a long channel residence time, and few scars whereas deltas with low ξ values are river dominated, have a short channel residence time, and numerous scars.

2.3 A test of the hypothesis

A goal of this thesis was to test the idea that waves suppress avulsions by using observational data from modern deltas. By using the morphology of the delta as well as the relationship between wave energy and sediment input, I endeavored to correlate the shape of the delta with the avulsion frequency. This entailed looking at deltas with different amounts of wave energy and determining the number of avulsions on each. In conjunction with that, I also looked at the spatial distribution of avulsions to determine if they are confined to a particular part of the delta surface or,

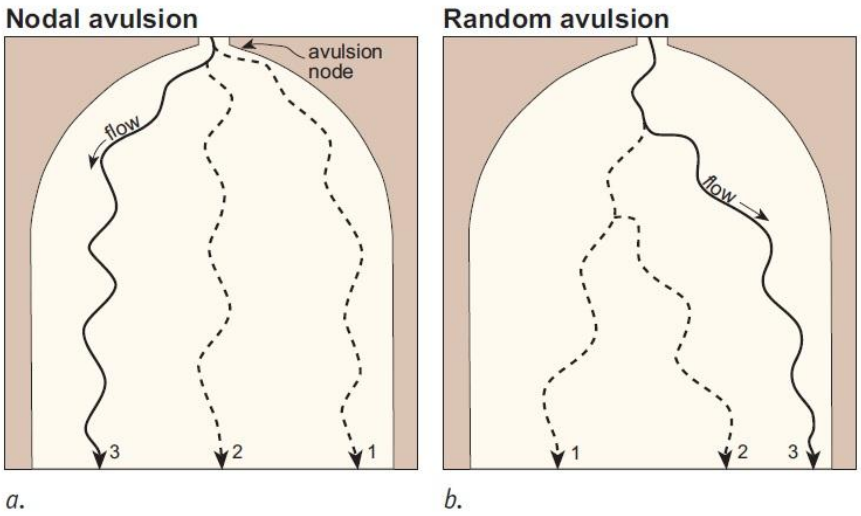

Figure 18. Leeder (1978) defined a. a nodal avulsion and b. a random avulsion (Gouw, 2007).

instead, if avulsions operate everywhere on the delta surface. In order to create the Swenson (2005) model, an assumption was made that simplified the delta geometry by only considering a single distributary channel that avulsed in a 'nodal' sense (Figure 18). If though, the super-elevation theory for avulsions is correct and avulsions have the ability to occur anywhere on the delta surface – random avulsions – I should be able to map the avulsion distribution to test the theory.

In order to directly test the Swenson (2005) model, the aforementioned river and wave parameters would have to be measured for various deltas. The avulsion frequency for these same deltas would have to be determined and the resulting data could then be plotted along with the predicted results from Swenson (2005) (Figure 17). However, measuring sediment input and wave energy in a deltaic system is fraught with uncertainty. Humans have dammed rivers, deforested watersheds, and farmed delta surfaces, drastically changing the sediment load in the (geologically) recent past. Sediment-load data are simply unavailable for a majority of the world's deltas. The relationship between wave energy and longshore drift is extremely difficult to quantify, particularly on longer (decadal or greater) timescales. General wave height and incidence angles have been

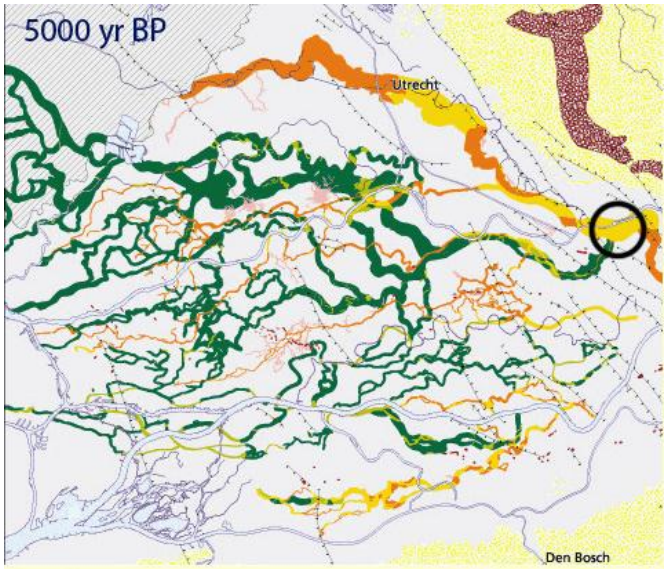

Figure 19. Map of ancient channels on the Rhine-Meuse delta (Berendsen & Stouthamer 2001).

measured for some systems on short timescales (Wang et al, 1998), though most transport is likely to occur during large storm events, which were probably not captured in these short-term observations. Some measurements of longshore drift have been attempted, but they do not fully cover the intricacies of sediment motion. These difficulties suggest that an alternative approach should be considered to construct a proxy for avulsion frequency.

The internal dynamics of avulsions are very intricate and poorly understood. Avulsions are a stochastic process and in order to achieve an effective understanding of avulsion frequency, data have to be averaged over a statistically significant number of avulsions to accurately describe the processes at work. As studies of Holocene deltas have suggested that large-scale avulsions occur on timescales of centuries to millennia (Slingerland and Smith, 2004; Tornqvist and Bridge, 2002), measuring them on human timescales is impracticable. Given these infrequent and unpredictable timescales, acquiring a statistically-significant number of avulsions to achieve a reliable time-averaged avulsion frequency requires using the stratigraphic record. This process entails widespread coring of deltas that have a long history of avulsions and then mapping the avulsions (Figure 19). The stratigraphic architecture this provides (Figure 20) results in time averaging of the avulsion frequency. Systems where this method has been

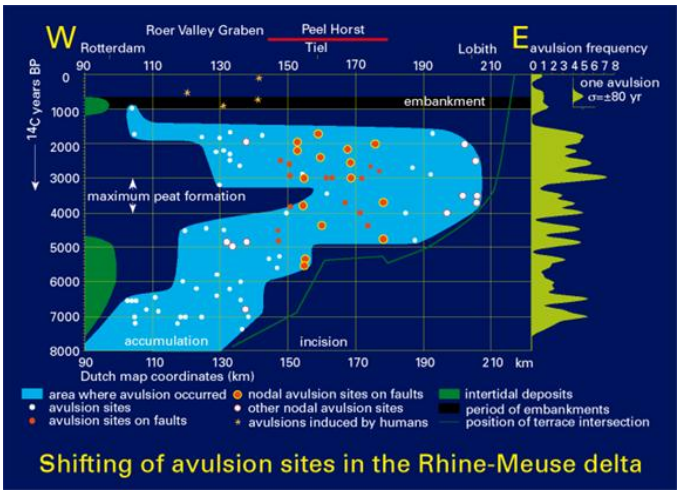

Figure 20. Stratigraphic architecture - specifically of avulsion locations - from the Rhine-Meuse delta (Stouthamer, 2001).

applied include the Rhine-Meuse and Mississippi deltas (Stouthamer, 2001; Tornqvist and Bridge, 2002), though only the Rhine-Meuse system has been mapped to the extent necessary to perform the time averaging required to determine an avulsion frequency.

Using the ancient stratigraphic record to produce a time-averaged avulsion frequency is not a feasible option. It is an extremely costly and time-consuming process. Furthermore, in order to test the ability of waves to suppress avulsions, numerous deltas from a wide range of relative wave energies would have to be cored and mapped to an extensive degree. Instead, I propose to average over space instead of time, loosely borrowing from the field of statistical mechanics. I suggest using the idea of **ergodicity** to measure avulsion frequency for a set of modern delta surfaces rather than from the stratigraphic record.

2.4 Ergodicity

An ergodic system is one in which temporal averaging can be interchanged with spatial averaging (Figure 21). My plan applies this approach to modern deltas. Instead

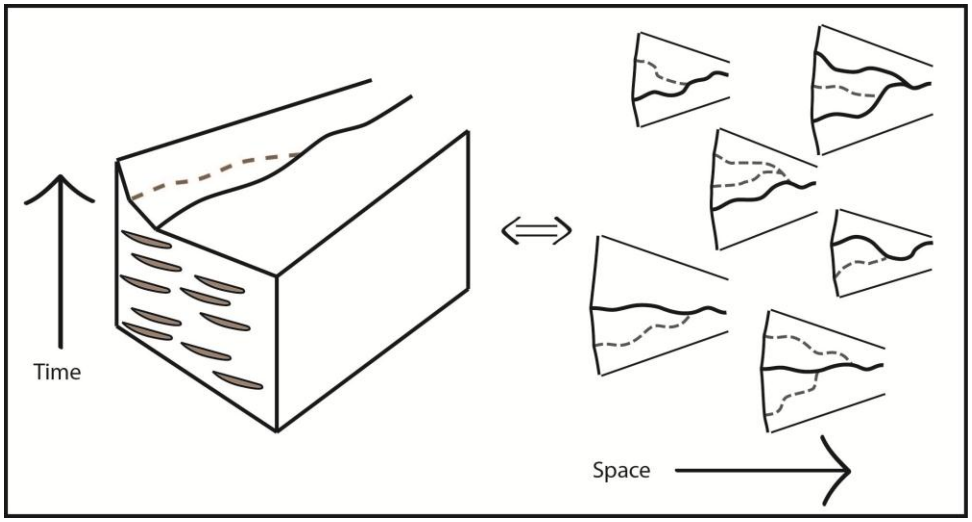

Figure 21. Schematic illustrating the principle of ergodicity - swapping temporal averaging with spatial averaging.

of measuring avulsions on a single delta through time, which requires using the underlying stratigraphic record, we can map avulsions on many 'identical' deltas at one point in time, i.e. now. In principle, for this method to work, we need to identify a set, or 'ensemble' of deltas with identical river and wave parameters; they need to have identical ξ values. In practice, we can create ensembles of deltas that have *similar* ξ values and average over each of these groups. By using the idea that ξ controls both the morphology of the delta and its avulsion frequency, modern deltas can be grouped into ensembles of similar wave influence based on their shape. Each delta within a given ensemble will not have exactly the same ξ value as the rest, but they will be similar enough to produce bulk results, which are all that can be expected when measuring stochastic systems.

Looking at systems at one point in time – the present – requires we have some method of observing the locations of avulsions in the recent past. We determined that channel scars provide this relationship as they are the remains of previous channels preserved in the deltas surface and have not yet been filled in, or annealed, by floodplain processes. Mapping (counting) the channel scars produces an avulsion frequency for that particular delta: For a given rate of floodplain annealing, a delta with many channel scars on its surface has a larger avulsion frequency than does one with few scars. By averaging across all the deltas within a specific ensemble, we produce an overall avulsion frequency for that ensemble, which is equivalent to measuring the avulsion frequency for that value of ξ. Through this approach, we can test the idea that waves suppress avulsions. The different ensembles represent different values of ξ. If the theory is correct, we should observe a systematic decrease in the average avulsion frequency for a given ensemble with increasing ξ value for the ensemble. For example, the ensemble corresponding to

deltas with a large amount of wave energy and correspondingly smooth and cuspate morphologies should show relatively few avulsion scars and thus a low avulsion frequency.

This method does make a few assumptions in order to simplify the model. To classify the deltas into the appropriate ensembles, we had to look at each delta and pick a category in which it best belonged. In order to minimize any bias, multiple people separately classified the deltas and the results were combined and any disputed deltas were further examined. All deltas have also started becoming more wave-dominated in recent years due to humans affecting the sediment supply through dams. These effects can be seen at the edges of the deltas, but overall the systems retain their previous morphology and our classifications are based on the former profile. As with any type of approach to science, our method has some limitations, but also like other approaches, they can be worked around and in this case, do not affect the overall outcome of the study.

3. Methods

3.1 Observational methodology

One hundred sixteen deltas were selected from a Google Earth global database of over fourteen hundred marine deltas (database complied by Doug Edmonds [Indiana University] and Sarah Baumgardner [St. Anthony Falls Laboratory]) and determined suitable for mapping based on the following criteria: minimal tidal and human influence, sufficient image resolution to make out channel scars, and at least one relict (scar) or

current avulsion (bifurcation). Once selected, the deltas were categorized into one of four classifications based on the observed amount of wave energy, or the morphology, of the delta (Figure 22). This classification used the basic definition of the Galloway diagram (Figure 7) and focused specifically on the river-wave leg of the diagram. I excluded deltas with large amounts of tidal influence as they are more prone to have complicated channel bars and tidal channels and, potentially, the effects of tides on the boundaries of the delta could dominate the impact of avulsions for a substantial fraction of the delta surface. As this categorization of the deltas was a subjective exercise, multiple people independently classified the deltas and any conflicting images were carefully reassessed. Classification # 1 includes the strictly river-dominated deltas which have channel tips protruding into the body of water. Deltas that still have the radial symmetry of the river-dominated systems but have lost their channel tips were placed into classification # 2. Deltas that showed a cuspate formation instead of the radial symmetry went in classification # 3. The fully wave-dominated systems, those that displayed a completely wave-smoothed front, were put into classification # 4.

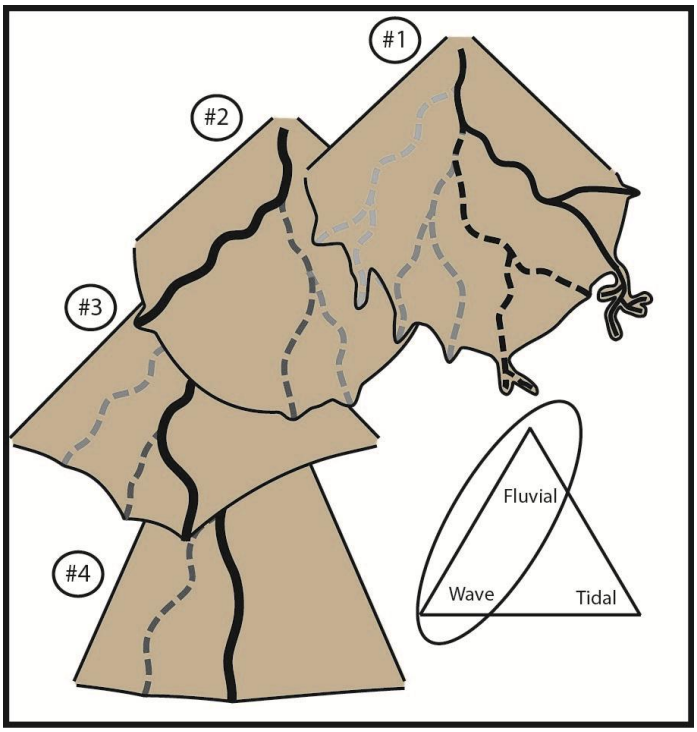

Figure 22. Morphologic classifications used to bin the deltas according to their relative wave energy.

Once classified, boundaries were set to delineate the outside margins of each delta. The point at which it was necessary for the main channel to begin avulsing in order to cover the entire delta surface was determined to be the apex. An east and west flank were marked as being the farthest longitudinal extent of the delta (Figure 23A) and the angle between them was termed the opening angle. Each system was then mapped for its avulsion nodes. An avulsion node was defined to be any point at which the channel splits and does not rejoin itself farther down the delta surface. To determine the nodes, every channel – including both active and relict channels – was traced (Figure 23B) and the points at which channels separated were marked (Figure 23C). Each delta was different in size and in order to compare the statistics, they had to be normalized. Three different length scales were used to normalize the data; all gave comparable results. One length scale was merely the maximum length from the apex to shore (R_{max}). Another was an average length scale created by averaging

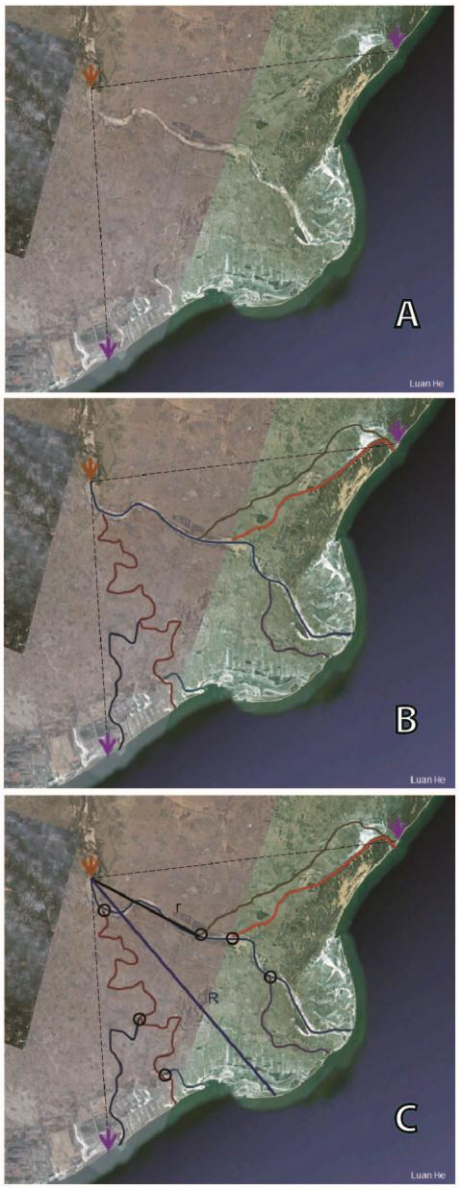

Figure 23. An example of the methods employed to map a delta. A) The apex and flanks of the delta were determined B) each channel was traced and C) the nodes marked and distances normalized.

distances from the apex to shore in multiple directions (R). The final length scale was calculated by determining the area of the delta and taking the square root of it (ℓ), which gave an order of magnitude estimate.

The density of scars on a deltas surface provides a direct measure of avulsion frequency. Counting the number of scars on the surface provides the number of times the channel has avulsed during the time it takes for the delta to heal or anneal these relict channels. By making the assumption that each delta has a similar annealing time, the number of scars over the entire surface of a delta is directly proportional to the delta averaged avulsion frequency. This assumption can be justified by looking at the 'big picture': I am looking at the deltas at a single point in time (the modern), thus, they have all been influenced by the same changes in eustatic sea level. The majority of these deltas are situated on passive margins with a minimal amount of subsidence, which means they have similar changes in relative sea level. Changes in relative sea level are an important part of what drives deposition on a delta as the first priority of the distributary channels is to maintain the surface of the delta at sea level and thus prevent it from drowning. Therefore, the similarities in changes in relative sea level between the deltas can potentially be extended to include the annealing time as well. In other words, the annealing time, which depends on the floodplain deposition rate, is mainly controlled by changes in relative sea level; because the variation in relative-sea-level change is likely small between the deltas I analyzed, it is probably reasonable to assume relatively little variability in the annealing time between deltas.

The database of mapped deltas was sorted according to several variables other than just wave energy classifications in an effort to discover any relationships that might

exist. Three additional properties – latitude, opening angle, and size of the delta – were considered and each was divided into three categories. Latitude classifications were defined as 0-30°, 30-60°, and 60-90°; I did not distinguish between deltas in the northern and southern hemispheres based on the idea that the climates in each of the cells are similar regardless of the hemisphere it is in. Opening angle definitions were broken up into deltas that had an opening angle of less than 60°, ones with an opening angle between 60-90°, and ones that had an angle larger than 90°. Size classifications were also placed in bins of less than 100 km^2, between 100 – 1000 km^2, and greater than 1000 km^2. Both the opening angle and size categorizations were qualitatively chosen after looking at the collected data to determine obvious groupings.

3.2 Sources of uncertainty

Fundamentally, my thesis represents a mapping exercise, and, like all mapping, there is a subjective aspect to the methods. The following are some points at which uncertainty could have been introduced to the results and some ways in which I attempted to mitigate that uncertainty. As I have already mentioned, the classification of the deltas into bins based on their morphology has the potential to be biased. We endeavored to lessen the bias by *independently* classifying the deltas and removing any that were questionable. In total this amounted to a handful of deltas that we could not classify without dispute. Another source of error is the resolution of the images I was using. Google Earth has images from all over the world, but the quality of those images varies based on location. I used only images that were clear, and when some feature was vague

or indistinct, I sought a second opinion on my interpretations. The simple act of differentiating active from relict channels on a delta surface is surprisingly difficult. At high flow conditions or during wet seasons, many relict channels are flooded and do not appear altogether different than active channels. At moderate to low flow conditions, the point bars of active channels are quite prominent in satellite imagery. Humans have occupied deltas for centuries due to the ease of farming on their surfaces and in doing so, have modified the natural channels. I culled any deltas that showed extensive reworking by humans, but almost all showed at least a few signs of human interference. I excluded any avulsion nodes that were obviously modified. It is worth noting that in some cases, human activity actually helped in finding relict channels. Examples include the construction of buildings on the topographically high channel levees and dredging of relict channels for navigational purposes. The measurement of down-delta distances is affected by the resolution of Google Earth and where I determined the apex of the delta to be. The determination of the apex is another subjective exercise, but as it was defined using an objective set of criteria, it is unlikely to introduce significant error to the statistics.

4. Results

4.1 General trends

The one hundred sixteen deltas that I mapped for this project span the previously described set of four different wave classifications or ensembles (Figure 24). Due to the rarity of truly river-dominated systems though, there are only a few deltas in

classification #1. This has the potential to skew the statistics for this particular bin by averaging over an insignificant number of deltas. There is a decreasing trend in the number of deltas in bins 2 through 4 with classification #2 having over twice as many deltas as classification #4. However, the number of deltas in each of the other three bins is a sizable amount, suggesting the statistics for these classifications will be robust.

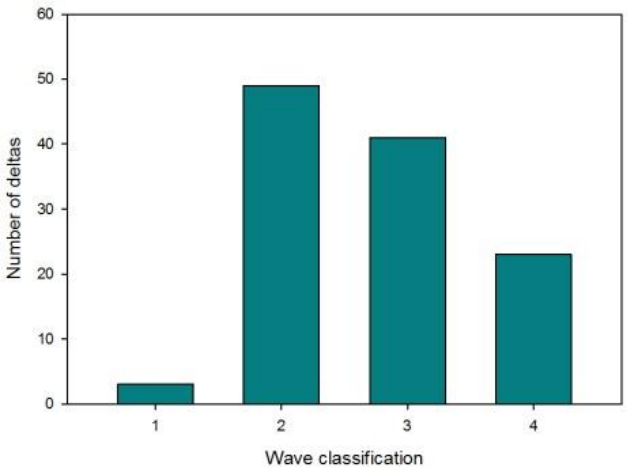

Figure 24. Total number of deltas in each wave classification ensemble.

Locations of the mapped set of deltas on a global scale were defined by their latitude. Each hemisphere – north and south – was divided into three equal sections of latitude with 0-30° corresponding to the equatorial regions, 30-60° the temperate, and 60-90° the polar regions. The deltas were not delineated between being in the northern or southern hemisphere. As Figure 25 shows, the majority of the deltas are located in the equatorial regions and the numbers decrease with an increase in latitude. The locations of the deltas were then sorted

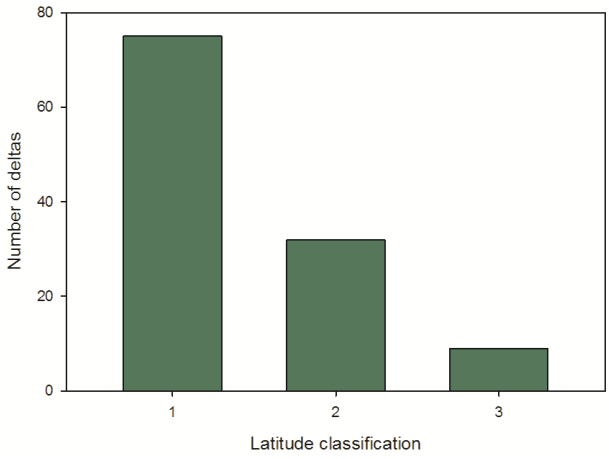

Figure 25. Total number of deltas in each latitude classification.

according to wave classification (Figure 26). No strong correlation between wave classification (ensemble) and latitude exists. There is a weak trend of the more river-influenced systems in the lower latitudes while the higher latitudes have a few more of the wave-dominated systems. It is important to note that this latitudinal distribution applies only to the set of deltas that was mapped and not to the world's deltas in general.

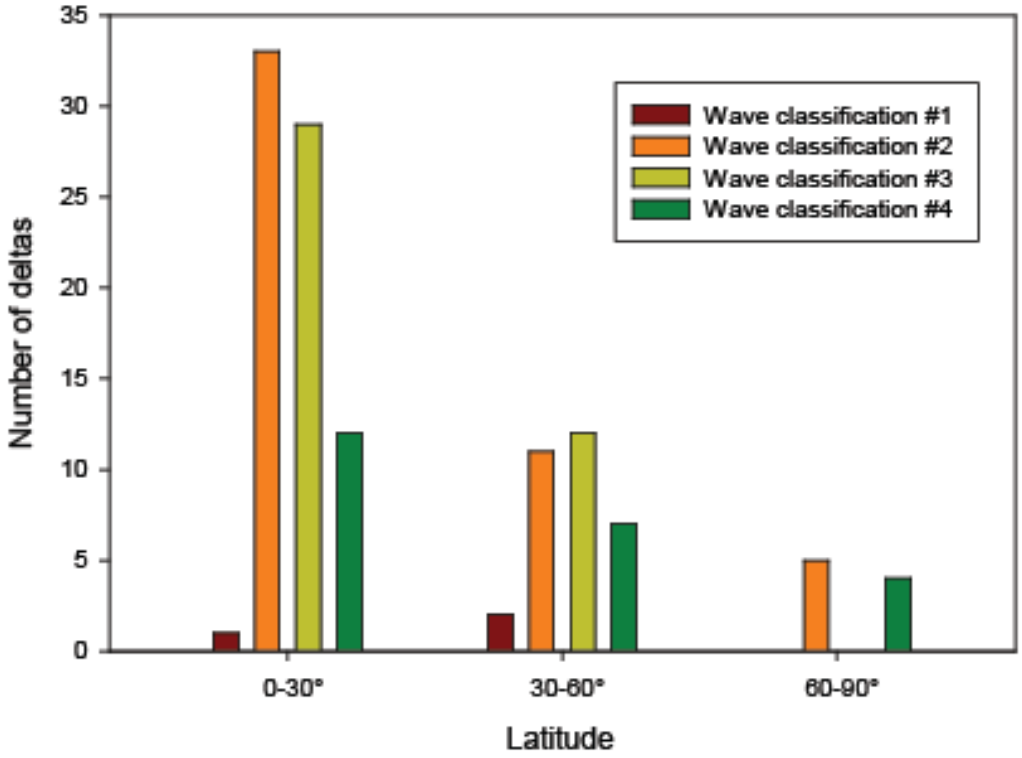

Figure 26. Number of deltas in each wave classification for each latitude group.

Larger deltas might be expected to have more avulsions simply due to their larger surface area (topset). As such, an ensemble populated with disproportionately large deltas might yield a relatively large avulsion frequency on the basis of delta and not wave influence. To address this possibility, I analyzed the distribution of delta size within each ensemble; my statistics are shown in Figure 27, where R_{max} is used as the length scale to

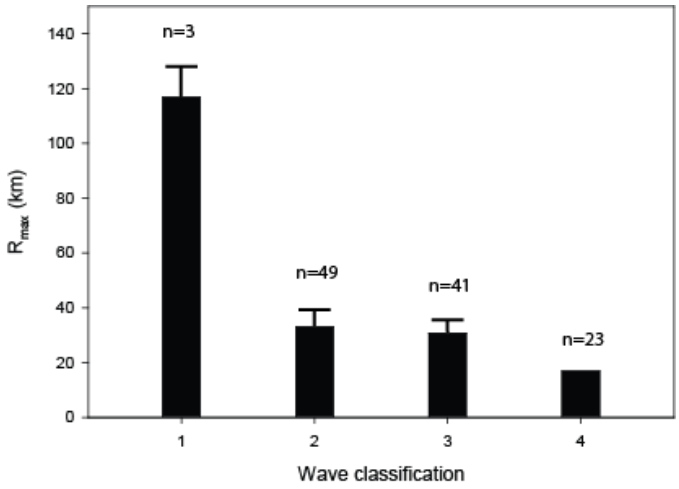

Figure 27. Average R_{max} for each wave classification along with the standard deviation in size for each bin.

describe the size of the delta. With the exception of wave classification (ensemble) #1, the mean delta size does not vary significantly between ensembles. The anomalously high average length scale that can be seen in wave classification #1 is due to the Mississippi River delta, which is included in that classification. The Mississippi is much larger than any of the other deltas in that classification, and is, in fact, the largest delta I mapped. Classifications #2 through #4 show a slight decrease in size as wave influence increases. The standard deviation of the size of the deltas within each wave classification was also determined. Wave classification #1 has a high variance in average R_{max} because of the vastly different sizes of deltas, implying the statistics that result from these deltas are suspect and should be considered as such. The variance decreases with increasing relative wave

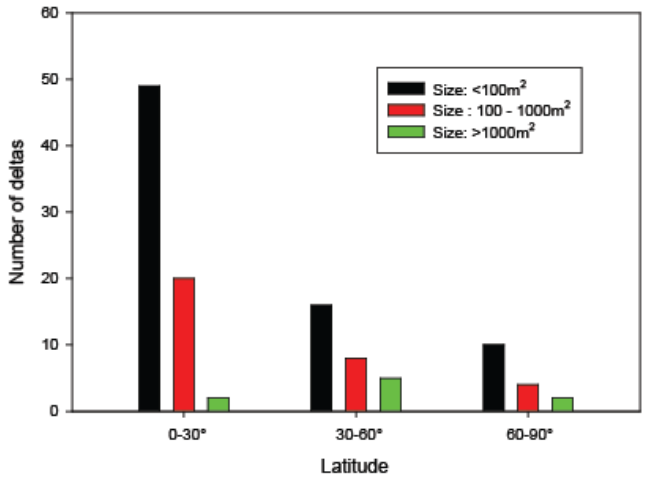

Figure 28. Number of deltas in each size classification for each latitude group.

influence which suggests the size of the deltas are more uniform when the systems are experiencing more relative wave energy. Overall, most small deltas (less than 100 m^2) are found at lower latitudes and that number decreases with increasing latitude (Figure 28). This trend is also seen in the medium sized-deltas (between 100 m^2 and 1000 m^2) while the larger deltas (greater than 1000 m^2) are distributed fairly evenly across all latitudes, with just a few more seen in the mid-latitudes than in either of the other two groups.

4.2 Bulk avulsion frequency vs. relative wave energy

A primary goal of this study was to test the idea that an increase in relative wave energy reduces the avulsion frequency. This means that more relative wave energy would create a delta surface that has fewer relict channels. I sorted the mapped deltas

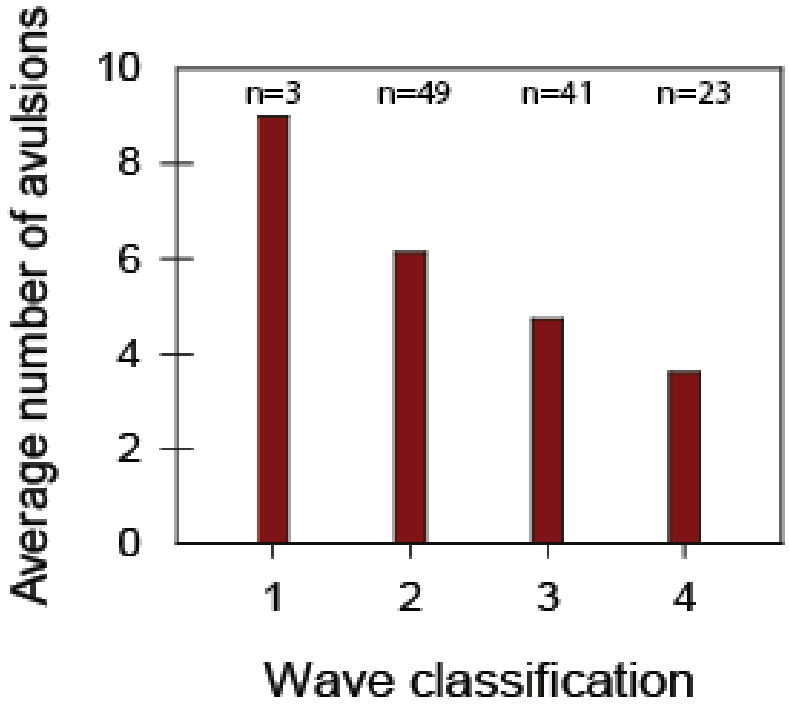

Figure 29. Bulk distribution of avulsions based on wave classifications, numbers correspond to the number of deltas within each ensemble.

into the different wave classifications (ensembles) by using their morphologies as the method of delineation. Separating the systems based on shape is qualitative, but ties directly to the amount of relative wave energy influencing the system. Based on this method of classification, there are only a few deltas in the river-dominated group.

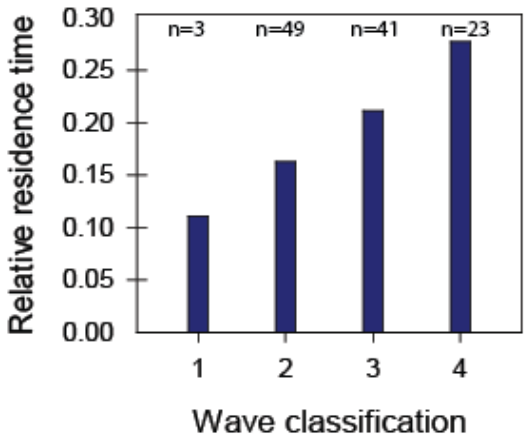

Figure 30. Residence time for the deltas as a function of wave classification plotted in the same format as the prediction of the model, numbers correspond to the number of deltas within each ensemble.

My results for the bulk distribution of avulsions can be seen in Figure 29, which shows the average number of avulsions per delta in each ensemble. The average number of avulsions is a proxy for the avulsion frequency, i.e. it is a 'relative' avulsion frequency. I computed this average by summing the total number of avulsions for all deltas within an ensemble and then dividing by the number of deltas in the ensemble. Statistics for these data are in Table 1. An alternative approach was also used to compute the avulsion density. I created a density for each delta by dividing the number of avulsions by the maximum length scale, and then averaged these within each bin. The results from this

Classification	**1**	**2**	**3**	**4**
Number of deltas	3	49	41	23
Number of avulsions	27	301	194	83
Average number of avulsions	9.0	6.1	4.7	3.6
Standard deviation	2.9	8.0	5.3	2.7

Table 1. Statistics regarding the bulk avulsion frequency for each wave classification.

method did not differ significantly from the original method of simply averaging the number of avulsions with the number of deltas. While the true average of avulsions for wave classification #1 is uncertain due to the low number of deltas in the ensemble, the overall trend in bulk avulsion frequency remains the same if it were to be removed. Another way of portraying the avulsion-node data is to consider the channel residence time, τ, which scales as one over the number of avulsions (Figure 30) and follows well with what the model predicts (Figure 17). The model suggests that the channel residence time increases nonlinearly with an increase in wave energy which can also be seen in the measured data.

4.3 Spatial distribution of avulsions

According to the hypothesis by Jerolmack and Swenson (2007), if super-elevation is the driving cause of avulsions, then an avulsion could occur anywhere on the surface of a delta. Based on their analysis which focused on lengths of active channels and did not include relict channels or nodes, they were unable to characterize the spatial distribution of where avulsions occur and, thus, if this hypothesis holds. In short, their findings suggested that avulsions were focused near the delta apex. In my study, I explicitly measured the downstream distance to both relict and active avulsion nodes (Figure 31) as well as their azimuthal

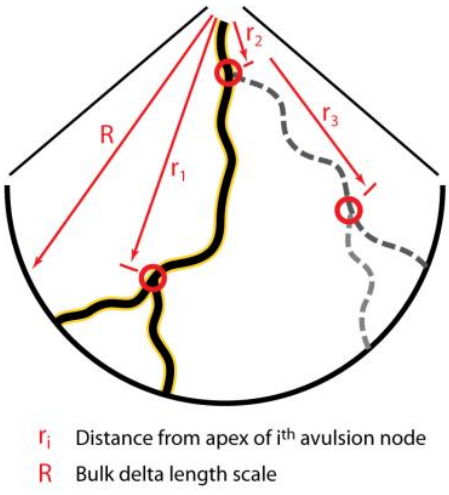

Figure 31. Schematic illustrating the down-delta distance to various nodes and the azimuthal averaging this study entails.

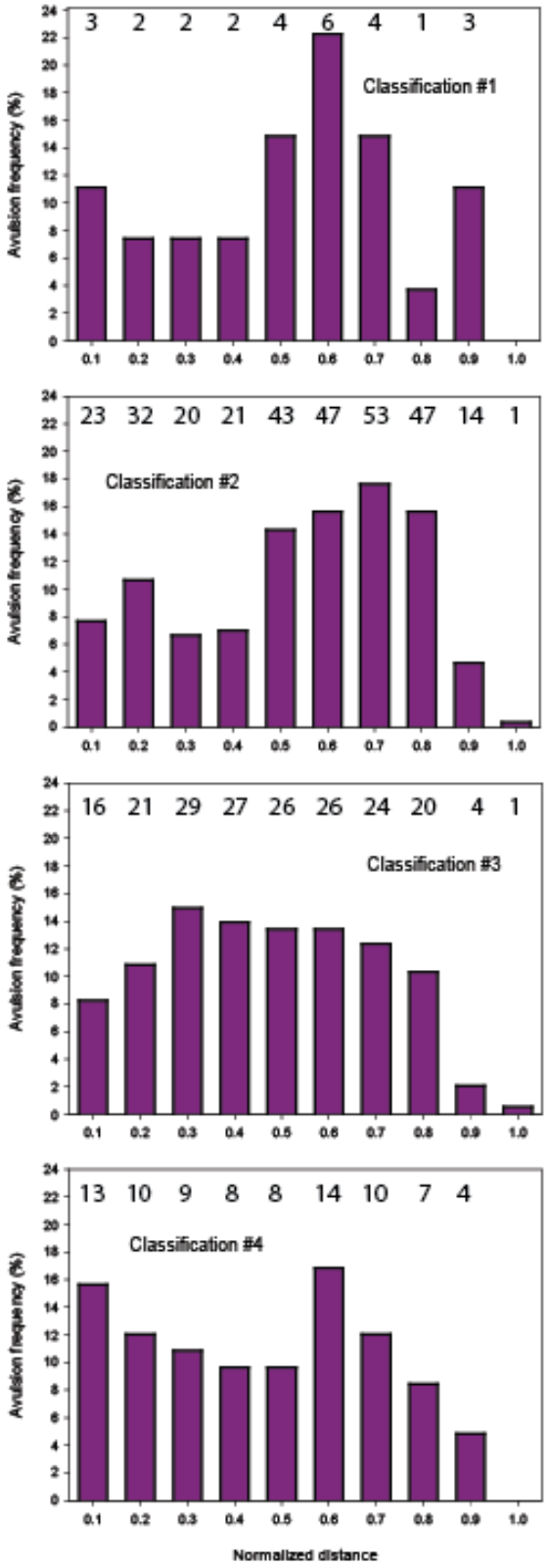

angle. In these results (Figure 32), these data are averaged over the azimuthal angle, which means that I am only looking at the radial component. I used the same wave classifications for the spatial distribution data as I did for the bulk density with classification #1 being river-dominated and classification #4 being wave-dominated. I normalized the down-delta distance to each node by R_{max} – the maximum radial distance for a given delta – and grouped the resulting data into bins of dimensionless 'length' 0.1. The basic differences between ensembles illustrated in Figure 32 are insensitive to the bin size and the statistics of each classication are in Table 2.

Overall, regardless of relative wave energy, my data sugggest that the avulsion process does indeed operate

Figure 32. Spatial distribution results of avulsion frequency vurses down-delta distance for each of the four wave classifications, numbers correspond to the number of avulsions within each bin.

across the entire delta surface; in contrast to the observations of Jerolmack and Swenson (2007), the avulsion process is not restricted to the delta apex region. In addition, these data show a few notable trends based on relative wave energy. In systems with low relative wave energy – classification #1 – the avulsions appear to have a maximum in the downstream region of the delta, relatively near the shoreline (Figure 32a). This location of the maximum number of avulsions shifts 'up' the delta and has less of a distict maximum with increasing relative wave energy. In the wave-dominated systems – classification #4 – the avulsions appear to be more randomly distributed without an overall clear trend (Figure 32d). Despite the fact that these results are limited to the resolution of my data and the relatively few deltas I was able to include in my study, they show the same sorts of trends regardless of what bin size is used to group the data.

Classification #1 (N=3 deltas)										
Bin	0.1	0.2	0.3	0.4	0.5	0.6	0.7	0.8	0.9	1
Number of nodes	3	2	2	2	4	6	4	1	3	0
Frequency	11.11	7.41	7.41	7.41	14.81	22.22	14.81	3.70	11.11	0.00
Ensemble average	1.00	0.67	0.67	0.67	1.33	2.00	1.33	0.33	1.00	0.00
Standard deviation	0.00	0.47	0.94	0.47	1.89	0.82	0.47	0.47	1.41	0.00
Classification #2 (N=49 deltas)										
Bin	0.1	0.2	0.3	0.4	0.5	0.6	0.7	0.8	0.9	1
Number of nodes	23	32	20	21	43	47	53	47	14	1
Frequency	7.64	10.63	6.64	6.98	14.29	15.61	17.61	15.61	4.65	0.33
Ensemble average	0.47	0.65	0.41	0.43	0.88	0.96	1.08	0.96	0.29	0.02
Standard deviation	0.70	0.92	0.81	0.81	1.67	1.96	2.16	1.41	0.61	0.14
Classification #3 (N=41 deltas)										
Bin	0.1	0.2	0.3	0.4	0.5	0.6	0.7	0.8	0.9	1
Number of nodes	16	21	29	27	26	26	24	20	4	1
Frequency	8.25	10.82	14.95	13.92	13.40	13.40	12.37	10.31	2.06	0.52
Ensemble average	0.39	0.51	0.71	0.66	0.63	0.63	0.59	0.49	0.10	0.02
Standard deviation	0.58	0.59	0.83	1.59	1.01	1.12	1.06	1.04	0.30	0.15
Classification #4 (N=23 deltas)										
Bin	0.1	0.2	0.3	0.4	0.5	0.6	0.7	0.8	0.9	1
Number of nodes	13	10	9	8	8	14	10	7	4	0
Frequency	15.66	12.05	10.84	9.64	9.64	16.87	12.05	8.43	4.82	0.00
Ensemble average	0.57	0.43	0.39	0.35	0.35	0.61	0.43	0.30	0.17	0.00
Standard deviation	0.58	0.50	0.87	0.48	0.56	0.71	0.71	0.62	0.48	0.00

Table 2. Statistics regarding the avulsions within each wave classification and down-delta bin.

5. Discussion and conclusion

My observations show a robust relation between avulsion frequency and relative wave energy on modern deltas (Figure 29). The bulk density of avulsions shows a decrease in avulsion frequency correponding to an increase in relative wave energy as waves remove a significant proportion of the sediment alloted to sedimentation (aggradation and progradation) of a distributary channel. In a gross sense, my findings support (or fail to refute) the hypothesis of Swenson (2005), providing observational evidence that increasing the amount of relative wave energy increases the amount of sediment being removed from the system. This, in turn, increases the amount of time necessary for a channel to super-elevate and avulse. Given my results and the fact that the avulsion frequency of a given delta as well as the morphology of the delta are a function of how much relative wave energy is acting on the system, the two appear to be able to be linked and the morphology used as a proxy for the avulsion frequency.

As something to consider, the small number of deltas in wave classification #1, the classical river-dominated deltas, calls into question the apparently equal weighing of delta classes that is a characteristic part of the Galloway plot (Figure 7). My observations suggest that it takes a relatively uncommon set of circumstances to create a truly river-dominated delta, either a very large amount of sediment or a very sheltered location where waves cannot rework the edges of a delta. Such conditions appear rare in modern natural systems. While Galloway's ternary polt remains useful for highlighting the end-member delta morphologies, it seems that more emphasis should be placed on the observation that nearly all natural deltas show significant wave influence.

My observations of the spatial distribution of avulsions contradict those of Jerolmack and Swenson (2007). My findings would suggest that the avulsion process operates everywhere on the delta surface; avulsions are not restricted to the 'nodal' variety. Most likely, the contradiction arises from the different methodologies. Jerolmack and Swenson (2007) mapped only active channels and, in doing so, failed to use the additional information available on the delta surface in the form of relict channels.

While not overly robust or 'clean,' the spatial distibutions of avulsion nodes does show a dependence on relative wave energy (Figure 32). One possible explanation for the observed trend is that the spatial distribution of the avulsion nodes is influenced strongly by the increase in area a delta experiences along the length of the delta from apex to margin. Another way of putting it is that if the area of a delta increases with distance from the delta apex, then the distributary channels must avulse more rapidly with distance from the apex in order to distribute sediment across the delta surface. Modeling the surface of a delta as a wedge of a circle creates a linear relationship between the down-delta change in the area of the delta (ΔA) and the radius, $\Delta A \sim r\Delta r$. The simple model is best described using the river-dominated system and making the assumption that sedimentation balances

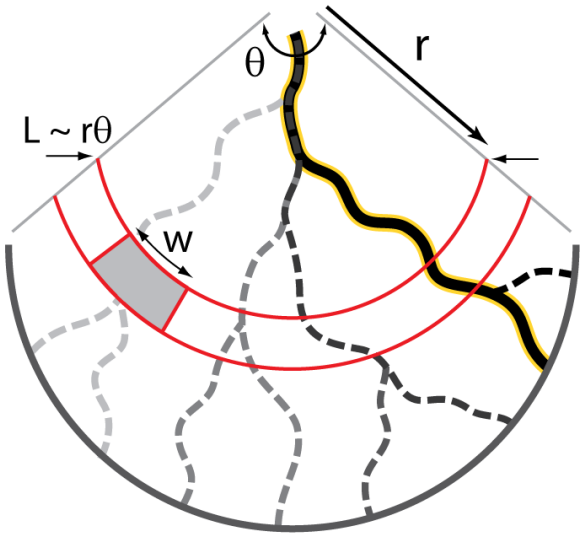

Figure 33. Schematic of a delta showing how channels must avulse more frequently as they are required to distribute sediment over a greater area.

subsidence. Figure 33 shows an idealized deltaic system where θ is the opening angle, w is the depositional footprint of a channel, and L is the arc length at any given radius, r. The depositional footprint is the effective width over which the channel's sediment, both sand and mud, are deposited; it is assumed to be much larger than the channel width. The cross-sectional area of a channel's footprint is given by:

$$A_{cs} = w\varphi \tag{11}$$

where φ is the depositional increment formed as a result of bulk sedimentation rate (R_{bulk}) and the channel residence time (τ)

$$\varphi \sim R_{bulk}\,\tau \tag{12}$$

The channel return time (T_r) – the amount of time before a channel will return to a specific location on the delta – is a function of the arc length and the number of footprints along that length:

$$T_r = \frac{L}{w}\,\tau \tag{13}$$

Using the assumption that the subsidence rate (σ) is balanced out by the average sedimentation rate – the delta does not drown – the above equations can be combined in the following manner:

$$\sigma \sim R_{avg} \sim \frac{\varphi}{T_r} \sim \frac{\varphi}{\left(\frac{L}{w}\tau\right)} \tag{14}$$

$$f = \frac{1}{\tau} \sim \frac{L\,\sigma}{w\,\varphi} \sim \frac{r\theta\sigma}{w\varphi} \tag{15}$$

Equation (15) suggests that the frequency of avulsions – the inverse of the channel residence time – *increases linearly* with an increase in the radius. In a river-dominated system, φ is not much different than the flow depth.

The above reasoning applies to a radial, river-dominated delta, where we would expect the avulsion frequency to increase approximately linearly with distance from the apex. This model would seem to capture some of the behavior in the first two panels of Figure 32, the least wave-influenced deltas.

The addition of significant relative wave energy disrupts this simple linear relationship. Waves can pin a channel in place – suppress avulsion – which leads to an increase in the thickness of the depositional package associated with the channel residence time (φ). In other words, the channel has to sit in a location for a longer period of time to counteract the removal of sediment by waves, which then provides more time for sediment to be deposited within the footprint to offset the effects of subsidence. As the thickness of the sediment increment gets larger, the frequency of avulsions is reduced. In essence, every delta can be thought of as a combination of a 'river' system and a 'wave' system. The river part leads to the linear down-delta increase in avulsion frequency; the wave part suppresses avulsion frequency. The apex of a delta is the

beginning of the river system while the shoreline marks the beginning of the wave system, with the two controls working their way toward the other. Theoretically, the effects of waves will die off with distance upstream from the shoreline. Thus, the point on the delta surface with the maximum density of avulsion nodes shifts closer and closer to the delta apex as the wave influence becomes more prevalent.

5.1 Implications

Wave energy is well known to play an important role in controlling the morphology of a delta; less well understood is the importance of wave energy in controlling the avulsion rates of distributary channels responsible for distributing sediment across the delta surface. The results of my study show that wave energy plays a major role in determining the avulsion frequency of distributary channels. Systems with relatively large amounts of wave energy – measured with respect to fluvial input – show fewer (overall) avulsions than do deltas with less wave energy; furthermore, in systems with relatively high wave energy, the spatial maximum in avulsion frequency appears to occur closer to the delta apex than it does in systems with less wave energy.

The results of my study can be used to predict the overall distribution of channel bodies in the subsurface, thereby making my findings of particular interest to the petroleum industry. The stratigraphic architecture of deltas with relatively little wave influence would have a relatively large number of channel bodies in the subsurface, i.e. a large volumetric channel density, as a result of the relatively short channel residence time (or high avulsion frequency). The opposite would be true of systems with relatively high wave influence, which would have a relatively small number of channel bodies in the

subsurface. Hence, my findings may be of use in predicting the relative proportion or density of subsurface channel bodies (reservoirs).

River-dominated systems have a higher sand to mud ratio within the body of the delta than do systems that are considered wave-dominated due to the larger channel density within river-dominated systems. This would imply they produce better reservoirs when buried, both in terms of abundance of channel bodies and the interconnectedness of the sand bodies. However, wave-dominated systems could be just as useful as reservoirs as long as the location of the sand bodies was established. The amount of sand coming into each systems is relatively similar – the ratio of sand to mud is not dependent on the wave energy working on the edges of the delta – so the sand in the wave-dominated systems must be deposited somewhere. Only a portion of it is deposited in the channel bodies while the rest is smeared along the edges of the delta by longshore drift. This longshore smearing of the sand creates sand bodies mimicking the shape of the delta and would, presumably, create acceptable reservoirs when buried. Thus, the actual volume of reservoirs produced by a given delta is only determined by the size of the delta and not by the wave climate affecting it. The difference would be in the location of these reservoirs within the delta; river-dominated systems would have reservoirs within the body of the delta itself, while the majority of the reservoirs found in wave-dominated systems would be nearer the edges of the delta.

My study also has implications for deltaic response to anthropogenic influence, including anthropogenic climate change. Overall, deltaic systems around the world are shifting to a more wave-dominated state via a several different processes. One process is the reduction of sediment being supplied to the deltas. Most rivers around the world have

been dammed for some hydroelectric power generation and/or flood management purposes; dams reduce the amount of sediment – particularly the sand-sized fraction – moving through the rivers by trapping it behind the dam structure. Proportionally more of the sediment that actually is being delivered to the delta has to be used to keep the delta surface from drowning. This reduction in sediment supply due to damming is compounded by the recent increase in the rate of rise in eustatic sea level, itself likely the results of anthropogenic climate change. Rising sea level acts in concert with subsidence to create space on the delta surface that must be 'filled' in order to maintain the delta surface near sea level. Hence, the ratio of wave energy to fluvial input, i.e. the dimensionless number ξ, is decreasing for most deltas worldwide as a result of damming and sea-level rise. This reduction in ξ reduces the progradation rate and thus the aggradation rate, which in turn reduces the avulsion frequency. A third process potentially influencing the trend toward more wave-dominated systems is the predicted increase in the frequency of large storm events in coastal settings due to anthropogenic climate change. While the actual mechanisms of longshore transport are still being determined, it has been hypothesized – and seems intuitively reasonable – that large storms have a greater influence on the movement of sediment along the shoreline a delta. My findings would suggest that an increase in the frequency of large storms would then potentially be followed by a decrease in avulsion rates. The net effect of these three processes – the reduction in sediment being supplied to the deltas due to damming, the increase in the rate of rise in eustatic sea level, and the predicted increase in frequency of large storms – is a drop in the average avulsion rate, which in turn leads to increased channel stability. My work indicates that channels are going to stay in one location for a

longer period of time due to the fact that it will take additional time to aggrade to the point of super-elevation. While it is tempting to apply my findings to individual deltas on short (human) timescales, one should do so with caution. It is important to remember that, in general, avulsion processes operate slowly relative to human timescales. Although the effects of anthropogenic perturbations to deltas may – in some ways – be realized now or in the very near future, these perturbations may take decades to centuries before becoming apparent as a control on avulsion frequency.

My study focused on using the avulsion history preserved on modern delta surfaces to test theoretical predictions. In my opinion, future work in this area will most likely be experimental and theoretical in nature. I have generated almost all of the observational data that can be accumulated with the information available to us now. Refinements in the quality of delta imagery are unlikely to alter my data set significantly: The large-scale channels and scars created by avulsion processes are, in general, detectable in existing satellite imagery for nearly all deltas worldwide; higher resolution images will highlight smaller-scale channels created (predominantly) by mouth-bar bifurcation, but this channel-forming process was not the focus of my work. Performing a direct test of theory, i.e. determining ξ values using quantitatively measured river and wave data would be an excellent step forward, but as was mention earlier, those data are unavailable and will continue to be unobtainable for the foreseeable future. Laboratory scale experiments, such as those performed by the Saint Anthony Falls group, may hold the promise for direct tests of theory, provided the significant 'scale effects' can somehow be overcome.

The data I collected can be used to create a predictive model for the spatial distribution of avulsion nodes. The Swenson (2005) model assumed that avulsions occurred only at the apex. My results show that avulsions are distributed across the delta surface and that this distribution appears to be influenced by the relative amount of wave energy. I constructed a simple model to explain, in a gross sense, how waves might influence the down-delta location of maximum avulsion frequency. Now that the locations of avulsions nodes are known, a forward model predicting the spatial distribution of avulsion nodes can be constructed. By creating such a model, the locations of avulsion nodes – and thus, the internal dynamics of avulsions – can be better predicted.

References

Ashworth, P. J., Best, J. L., Jones, M. (2004), Relationship between sediment supply and avulsion frequency in braided rivers, *Geology*¸32, 21-24.

Berendsen, H.J.A & E. Stouthamer (2001), Palaeogeographic development of the Rhine-Meuse delta. Assen: Van Gorcum, 270 pp.

Bryant, M., Falk, P., Paola, C. (1995), Experimental study of avulsion frequency and rate of deposition, *Geology*, 23, 365-368.

Cooper, J. A. G., and O. H. Pilkey (2004), *Longshore Drift: Trapped in an expected Universe*, *Journal of Sedimentary Research*, 74, 599-606.

Galloway, W. E. (1975), Process framework for describing the morphologic and stratigraphic evolution of deltaic depositional systems, *Deltas: Models for Exploration*, edited by M.L. Broussard, pp. 87-98, Houston Geol. Surv., Houston, Tex.

Gouw, M.J.P. (2007), Alluvial architecture of fluvio-deltaic successions: a review with special reference to Holocene settings, *Netherlands Journal of Geosciences*, 86-3, 211-227.

Hajek, E., Wolinsky, M. (2011), Simplified process modeling of river avulsion and alluvial architecture: connecting models and field data, *Sedimentary Geology*, 257-260, 1-30.

Heller, P. L., Paola, C. (1996), Downstream changes in alluvial architecture: An exploration of controls on channel-stacking patterns, *Journal of Sedimentary Research*, 66, 297-306.

Hoyal, D. C. J. D., Sheets, B. A. (2009), Morphodynamic evolution of experimental cohesive deltas, *Journal of Geophysical Research*, 114, F02009.

Komar, P. D. (1973), Computer models of delta growth due to sediment input from rivers and longshore transport, *Geological Society of America Bulletin*, 84, 2217-2226.

Komar, P. D. (1998), *Beach Processes and Sedimentation*, 544 pp., Simon and Schuster, New York.

Jerolmack, D. J., Swenson, J. B. (2007), Scaling relationships and evolution of distributary networks on wave-influenced deltas, *Geophysical Research Letter*,34, L23402.

Mackey, S. D., Bridge, J. S. (1995), Three-dimensional model of alluvial stratigraphy: Theory and application, *Journal of Sedimentary Research*, B65, 7-31.

Martin, J., Sheets, B., Paola, C., Hoyal, D. (2009), Influence of steady base-level rise on channel mobility, shoreline migration, and scaling properties of a cohesive experimental delta, *Journal of Geophysical Research*, 114, F03017.

Mohrig, D., P. L. Heller, C. Paola, and W. J. Lyons (2000), Interpreting avulsion process from ancient alluvial sequences; Guadalope-Matarranya system (northern Spain) and Wasatch Formation (western Colorado), *Geological Society of America Bulletin.*, 112, 1787-1803.

Paola, C. (2000), Quantitative models of sedimentary basin filling, *Sedimentology*, 47, 121-178.

Shanley, K. W., McCabe P. J. (1994), Perspectives on the sequence stratigraphy of continental strata, *American Association of Petroleum Geologists Bulletin*, 78, 544-568.

Sheets, B. A., T. A. Hickson, and C. Paola (2002), Assembling the stratigraphic record: Depositional patterns and time-scales in an experimental alluvial basin, *Basin Research*, 14, 287-303.

Slingerland, R., Smith, N. D. (1998), Necessary conditions for a meandering-river avulsion, *Geology*, 26, 435– 438.

Slingerland, R., and N. D. Smith (2004), River avulsions and their deposits, *Annu. Rev. Earth. Planet. Sci.*, 32, 257-285.

Stouthamer, E. (2001), Sedimentary products of avulsions in the Holocene Rhine-Meuse Delta, The Netherlands, *Sedimentary Geology*, 145, 73-92.

Stouthamer, E., Berendsen, H. J. A. (2007), Avulsion: The relative roles of autogenic and allogenic processes, *Sedimentary Geology*, 198, 309-325.

Swenson, J. B., Voller, V. R., Paola, C., Parker, G., Marr, J. G. (2000), Fluvio-deltaic sedimentation: A generalized Stefan problem, *European Journal of Applied Mathematics*,11, 433-452.

Swenson, J. B. (2005), Relative importance of fluvial input and wave energy in controlling the timescale for distrbutary-channel avulsion, *Geophysical Research Letters*, 32.

Swenson, J. B., S. Gupta, C. Paola, and D. Jerolmack (2010), Temporal and spatial scales of autogenic dynamics in linked fluvial-marine systems; AAPG Annual Convention, New Orleans, LA, April 11 – 14.

Tornqvist, T. E., (1994), Middle and later Holocene avulsions history of the River Rhine (Rhine-Meuse delta, Netherlands), *Geology*, 22, 711-714.

Tornqvist, T. E., and J. S. Bridge (2002), Spatial variation of overbank aggradation rate and its influence on avulsion frequency, *Sedimentology*, 49, 891-905.

U.S. Army Corps of Engineers, 1984. Shore Protection Manual. Washington, D.C.: Coastal Engineering Research Center, U.S. Government Printing Office.

Wang, P., N. C. Kraus, and R. A. Davis Jr. (1998), Total longshore sediment transport rate in the surf zone; field measurements and empirical predictions, *Journal of Coastal Research*, 14, 269-282.

Wright, L. D., and J. M. Coleman (1973), Variations in morphology of major river deltas as a function of ocean wave and river discharge regimes, *American Association of Petroleum Geologists Bulletin*, 57, 177-205.